Thermal (IR) and Other NDT Techniques for Improved Material Inspection

8 AUTHORS, INCLUDING:

Daniel Balageas
Ecole Nationale Supérieure d'Arts et Métiers
284 PUBLICATIONS **1,798** CITATIONS

SEE PROFILE

Vladimir Vavilov
Tomsk Polytechnic University
140 PUBLICATIONS **694** CITATIONS

SEE PROFILE

Christophe Pradere
Institut de Mécanique et d'Ingénierie de Bo…
64 PUBLICATIONS **269** CITATIONS

SEE PROFILE

Giovanni Maria Carlomagno
University of Naples Federico II
371 PUBLICATIONS **2,642** CITATIONS

SEE PROFILE

CrossMark

Thermal (IR) and Other NDT Techniques for Improved Material Inspection

D. Balageas[1] · X. Maldague[2] · D. Burleigh[3] · V. P. Vavilov[4] ·
B. Oswald-Tranta[5] · J.-M. Roche[6] · C. Pradere[7] · G. M. Carlomagno[8]

Abstract Thermal nondestructive testing (TNDT) may be considered to be a more widely applicable method than many traditional techniques, such as X ray, ultrasonic, eddy current, liquid penetrant, etc. It can be applied to both metals and non-metals containing subsurface defects such as cracks, foreign inclusions, disbonds, delaminations, variations in thermal properties, etc. This is especially true for composite materials, and TNDT is very appropriate for screening purposes. TNDT test results may be analyzed by advanced image processing algorithms. This paper provides a concise review of composite NDT using TNDT in combination with other inspection techniques, providing an opportunity for data fusion.

Keywords Thermal nondestructive testing ·
Infrared thermography · Data fusion · Vibrothermography ·
Ultrasonic testing · Induction heating

✉ X. Maldague
maldagx@gel.ulaval.ca

[1] I2M, TREFLE Department, UMR ENSAM 5295, University of Bordeaux, 33400 Talence, France

[2] Electrical and Computing Engineering Department, Université Laval, Quebec, QC, Canada

[3] La Jolla Cove Consulting, San Diego, CA 92117, USA

[4] National Research Tomsk Polytechnic University, 30 Lenina Av. 30, Tomsk, Russia 634050

[5] University Leoben, Peter-Tunnerstr. 25, 8700 Leoben, Austria

[6] Composite Materials and Structures Department, ONERA, 29 av. de la Division Leclerc, 92320 Châtillon, France

[7] I2M-TREFLE Department, UMR CNRS 5295, University of Bordeaux, 33400 Talence, France

[8] University of Naples Federico II, Ple. Tecchio 80, 80125 Naples, Italy

1 Introduction

A number of nondestructive testing (NDT) techniques such as X ray, ultrasonic, electro-magnetic, and thermal/infrared, inject some forms of energy, either waves and/or particles, through an object. Some of the energy is absorbed and the remainder of the energy is detected after passing through the object. If an appropriate NDT technique is used, the intensity of the energy varies when structural defects are encountered and the presence and location of the defects are revealed.

For decades, metals constituted the majority of NDT applications. Typical defects in metals include voids, cracks, and pores.

Defects that reach, or nearly reach, the surface of a metallic body can be effectively detected by liquid penetrant testing or induced eddy currents. Deeper defects in metals are typically detected by X rays or ultrasonic waves.

Composite materials, which are being used increasingly in high tech industries (such as aerospace, automotive, power production, etc.), pose challenges to the above-mentioned traditional NDT techniques because of the following: (1) X rays are only weakly absorbed by non-metallic materials; (2) ultrasound can be strongly dispersed, or absorbed, in composites; (3) eddy currents cannot be induced in non-metals; (4) liquid penetrant detects only flaws that are open to the surface and materials with porous surfaces, such as composites, cannot be examined.

Thermal/infrared (T/IR) NDT (or TNDT) is a diffusive process, in which the heat that propagates in a solid is attenuated in space and shifts in time. The differential equation that describes heat conduction is very different from those describing the propagation of X rays and/or ultrasound. Therefore, the TNDT process is closely related to the physics of heat conduction and infrared (IR) waves.

🌻 Springer

Table 1 Defects detected by NDT (adapted from ASTM E2533-09)

Defect	Acoustic emission	Computed tomography	Leak testing	Radiography radioscopy	Shearography	Thermography	Ultrasound	Visual NDT
Contamination		X		X			X	X
Damaged filaments	X	X		X				
Delamination	X	X			X	X	X	X
Density variation		X		X		X	X	
Deformation under loading					X			
Disbond					X	X	X	X
Fiber disbonding	X	X[a]				X	X	
Fiber misalignment		X		X		X		
Fractures	X	X		X		X	X	X
Inclusions		X				X	X	X
Leaks	X		X				X	
Loose or moving parts	X							
Microcracks	X	X[b]		X[b,c]	X		X	
Moisture		X		X[d,e]		X		
Porosity	X	X		X		X	X	
Thickness variation		X		X[f]	X	X	X	
Undercure							X	
Voids	X	X	X	X		X	X	

[a] Can detect after impact
[b] Depends on opening/size of crack
[c] Depends on angle of beam relative planar defect and opening
[d] Only in central projection
[e] Radioscopic mode
[f] For radiography

The milestone studies on active TNDT were performed in the 1960s by Green, who developed the technology for checking nuclear reactor fuel elements [1,2] and then reported by Beller for the inspection of Polaris A-3 rocket motor cases [3]. From the 1970s to the 1980s, thermal wave and pulsed TNDT procedures were established and thoroughly investigated [4–7]. In 1976 Carlomagno and Berardi [4] introduced the concept of lockin thermography. For more details on the history and basics of TNDT, the reader is referred to some review and original papers [8–15].

Since the end of World War II, the so-called "big five" NDT techniques have been: X-ray, ultrasonic, eddy current, magnetic particle and liquid penetrant [16,17]. However, when one considers the more recent field of the inspection of composites, TNDT should be included in this list. In some applications, such as the inspection of space vehicle thermal protection systems [18], it is regarded as the best technique to use.

2 NDT Techniques: Advantages and Disadvantages

It is beyond the scope of this paper to provide a detailed comparison of these complex NDT methods, as there are many requirements and limitations, which depend on both the technique and the application. Selecting the best technique(s) for an application may require an extensive analysis by a highly experienced NDT engineer. Some indications on choosing a proper NDT technique can be found in Table 1.

The features of NDT techniques that are used for the inspection of large composite structures are compared in Table 2. This is adapted and expanded from [19].

The table provides only some general guidelines.

All methods:

1. Have limitations. No single method works for every application.
2. Require skill, training, and certification (except tap/sonic testing)
3. Produce images (except tap/sonic testing)

Some methods

1. Can only be used from one side of a panel.
2. Require access to both sides of a panel.
3. Require testing both sides of a panel separately, especially when testing a thick panel, or a panel with a honeycomb (or other) reinforcement.
4. Can be used in through-transmission mode if desired.

Table 2 Comparison of NDT methods used for the inspection of composite materials (adapted from [19])

NDT method	Equipment cost	Scan rate	One (1) and/or two (2) inspection[a]	Special requirements	Limitations
TNDT (IR)	Moderate	Fast	1, 2	Non-reflective, High emissivity surface	Defect detectability decreases with increasing laminate thickness
Laser Shearography	Moderate	Fast	1	Reflective surface[b]	Defect detectability decreases with increasing thickness
Ultrasonic (UT)	Moderate	Slow	1, 2	Couplant required[c]	Porous materials such as Ceramic matrix composites.
Air Coupled UT	Moderate	Slow	1, 2	No couplant	Low frequency Low spatial solution Limited possible applications
Laser Ultrasonic	Very high	Slow	1, 2	No couplant Pulse echo	Very expensive Laser safety Surface treatment Not good for honeycomb panels
X-ray[d]	Moderate	Slow	2	Safety concerns	Not very good for composites[d]
TeraHertz	Moderate	Fast	1, 2	Used for low density materials including foam	Material limitations Conductivity issues Good sensitivity to moisture content
Tap (sonic) testing	Very low	Slow	1	Should only be used in quiet area. Hearing test for operators.	Non-quantitative, unreliable method Should not be used on anything important

[a] Some methods only work from one side and some methods only work with access to both sides (through transmission). Some methods can be used either from one side or from both sides

[b] Test surfaces need not be highly reflective, but must reflect light to a certain extent

[c] "Normal" large-scale ultrasonic C-scan testing uses a water-based couplant. This creates a problem for composite materials, as the couplant is absorbed by the part which must be dried in an oven or autoclave. This adds cost and processing time. Air-coupled ultrasonic systems exist and laser ultrasonic systems do not require a couplant, but both of these methods have other limitations

[d] X-ray has limited application for composite materials. X-ray generally does not show voids and other common composites defects. It may show FOD and trapped water, depending on concentration and material properties

5. Are difficult to use on parts with complex contoured surfaces especially with tight curvature radii.
6. Require surface treatments before testing.
7. Have safety requirements that increase cost or inspection time, or reduce convenience.

Table 2 is simplistic; the ratings of the effectiveness of the techniques are very subjective. There are wide variations in possible structures for each material system and also constraints on the inspection requirements. All of these factors must be considered before selecting an NDT method for a specific application. These are not included in the above table, as their inclusion would make the table extremely complex. These embrace:

1. Thickness of laminates, facesheets, rubber layers,
2. Thermal and mechanical properties of the laminate,
3. Density of components including honeycomb, foam, balsa, or rubber layers,
4. Types and sizes of defects that must be found,
5. Scanning rate required,
6. Excitation method that will detect the desired defects.

3 Thermal NDT Features

Choosing an optimum NDT method for a particular application is a multi-parametric decision that depends on the material to be tested, the defects that must be detected, equipment cost, scanning rate and other specific requirements of the end-user. Below, the basic features of TNDT are summarized.

Since heat conduction occurs in all solids due to a temperature difference, in principle, TNDT is a universal method that could be applicable to any material. However, it may be stated

that low-conductivity materials do not allow enough heat to penetrate deeply into a body, thus limiting the detectable defect depth. Highly-conductive metals possess a high heat diffusion rate. Therefore, temperature signal observation times for defects might be very short and temperature patterns will fade quickly. Other limitations may exist if temperature is recorded by IR thermography. Shiny and/or polished metals, due to their low emissivity, cannot be easily heated by radiant methods and they also emit a reduced amount of thermal radiation. However, inspection is possible on metallic components if a high-emissivity coating is applied to the surface (this is often referred as "black-painting") and when rapid transients do not exist. Black-painting is beneficial for two reasons: first, the energy absorption from radiant lamps by the inspected surface is maximized and second, the high infrared emissivity creates good thermal contrasts on the inspected surface. It is important to note that regardless of their visible color, all oil-based (and most other) paints generally have an emissivity of ~0.9 in the infrared bands.

However, unlike metals, composite materials, particularly those that include carbon (carbon fiber reinforced plastic or carbon/carbon composites), provide a very effective target for TNDT, due to their reasonable thermal conductivity and high emissivity.

There are two major constraints in defect detection by TNDT. First, defects, which generally (but not always) have a lower thermal conductivity than the host material, must produce a significant disturbance in the heat transfer, and second, they must be relatively large in the direction perpendicular to the propagation of the heat flux. In fact, thin but wide material discontinuities are typical targets for TNDT. Even 'kissing' defects (disbonds) can be detected by TNDT using lateral heating schemes. This could also be performed by applying ultrasonic stimulation, which causes significant internal friction and the dissipated energy is detected.

A stimulating process can be described with a particular temporal mathematical function. In most cases, flash (Dirac-pulse), square pulse (step-wise) or sinusoidal thermal waves (lockin) heating are used. Additionally, some attempts to find an optimal heating profile have been occasionally undertaken [20].

In most cases, TNDT (often implemented as an IR thermographic process combined with optical stimulation) is a non-contact process, including both heating and temperature detection.

Another important characteristic of TNDT is its rapid scanning rate, which is important in the inspection of large composite aerospace parts, whose area may be many square meters.

And finally, TNDT procedures are safe and may be used, in manufacturing facilities, laboratories, workshops, airport hangars, other large buildings.

'Classical' TNDT uses optical means of heating, such as quartz, Xenon and halogen radiant lamps, and lasers.

Other heating methods, such as convective (hot/cold air) heating/cooling, are generally limited to step heating because of the difficulty in achieving periodic convective heating. Also, it is difficult to achieve a quasi-uniform heat flux over the surface of a sample and it is difficult to accurately calibrate the convective heat transfer distribution over this surface.

A primary difficulty of using radiant heating is its dependence on surface optical properties of a material, which affects the amount of energy absorption. This disadvantage can be sometimes overcome by using mechanical stimulation, induction heating, or by heating with radiation in a different spectral domain, such as microwave or millimeter waves, than the IR spectral band used for imaging. Novel techniques, such as the aforementioned ones, result from the addition of a thermal technique (essentially IR thermography) to another physical phenomenon. Such a combination of techniques may be very beneficial. In one case, the two techniques are used independently and data fusion is employed to optimize the inspection. Some examples are given in Sect. 4. In another case, the two techniques are integrated and performed together (see Sect. 5).

Finally, convection cooling has been used successfully for certain applications [12]. For instance, when a component is already hot due to a manufacturing process, cooling the component with cold air jets may allow the detection of defects. This works well for qualitative detection in some applications. However, as stated above, quantitative evaluation is not possible because the cooling source is not well characterized.

Recently, a case was reported in which air bubbles trapped in a polymer seal were detected by cooling being provided by a line of air jets (at room temperature) directed onto the specimen right after a thermal bonding step process.

Another example of such a "cool approach" is shown on Fig. 1 for the case of the inspection of solar photovoltaic cells (crystalline silicon, not thin film amorphous silicon) to detect cracks. The approach was to generate a lateral thermal pulse across the cell using Peltier elements, one in cooling mode and the other one in heating mode. The thermal resistance created by a crack can then be "seen" readily in the recorded thermogram [21].

4 Combining Thermography with Another Method (Data Fusion)

4.1 Ground Penetrating Radar and Thermography

Some features of using visual and TNDT in combination with ground penetrating radar (GPR) technique are illustrated in Fig. 2 [22] (test results: courtesy W. Swiderski). A standard
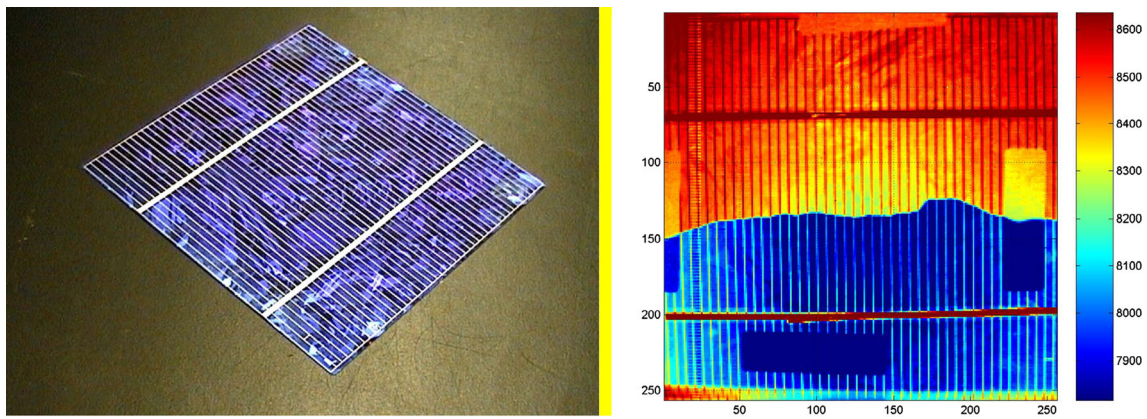
Fig. 1 Visible picture of a cracked solar cell (*left*). Raw temperature image of a cracked solar cell, arbitrary temperature units (*right*): *bottom* (cool) and *top* (warm) stimulation with Peltier elements are clearly visible (plastic tapes of different emissivity are seen on *left* and *right*)

(a)   **(b)**   **(c)**   **(d)**
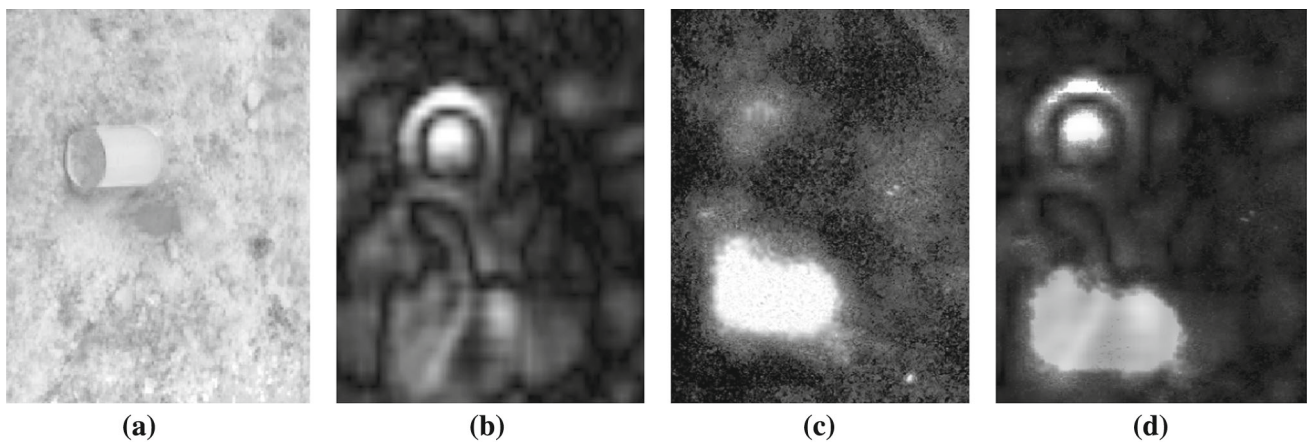
Fig. 2 Detecting a simulated landmine in the soil by combining visual, thermal and ground penetrating radar techniques [22]: (**a**) test site photo, (**b**) GPR image, (**c**) IR image, (**d**) fusion results (IR + GPR)

photo (Fig. 2a) shows only a can placed on the soil surface to imitate clutter while the simulated buried landmine is not visible. A predominant indication in the GPR image (Fig. 2b) is also affected by surface clutter. Instead, the IR thermogram of Fig. 2c taken at the best observation time clearly shows the simulated 'landmine' due to stimulation of the soil by solar radiation, while the can is barely visible, most probably because of the addition of the inherent and reflected IR radiation from the can. Image of Fig. 2d represents the result of fusion of the two previous images, combining indications of the clutter and the simulated 'landmine'.

4.2 X-rays and Thermography

Glass fiber reinforced plastic (GFRP), commonly known as fiberglass, is a good subject material for TNDT if the defect depth does not exceed a few millimeters, with the separation between laminas being in the micrometer range (Fig. 3a). X-ray computer tomography permits the analysis of very thin defects in the cross-section of a laminate, as shown in Fig. 3b

(X-ray energy 120 keV, minimum in-depth step 100 μm), but this technique is time-consuming and is difficult to apply to large components. TNDT may serve well as a screening inspection method for large areas (Fig. 3c).

Detecting water in aircraft honeycomb panels remains one of the most important problems in the maintenance of a modern air fleet. Standard X-ray radiography is probably the most sensitive NDT method for resolving water in a single honeycomb cell (Fig. 4a, left). However, this technique requires access to both sides of a panel, which is not always possible in practice. Other disadvantages are that the use of X-ray imposes strict safety requirements, and the quantitative evaluation of test results is difficult.

Again, IR thermography may well serve as a screening method (Fig. 4a, right). The IR image compares fairly well with the X-ray image and the sensitivity of TNDT is also capable of showing single honeycomb cells.

Quantitative evaluation of water content in aviation panels is typically done by ultrasonic NDT (UT), which measures the height of water in areas of a panel. But UT scans relatively slowly.

Fig. 3 Detecting disbonds in GFRP tube joints (adapted from [23]): **a** sample cross-section, **b** X-ray tomogram ("slice" image), **c** one-sided TNDT image of disbond
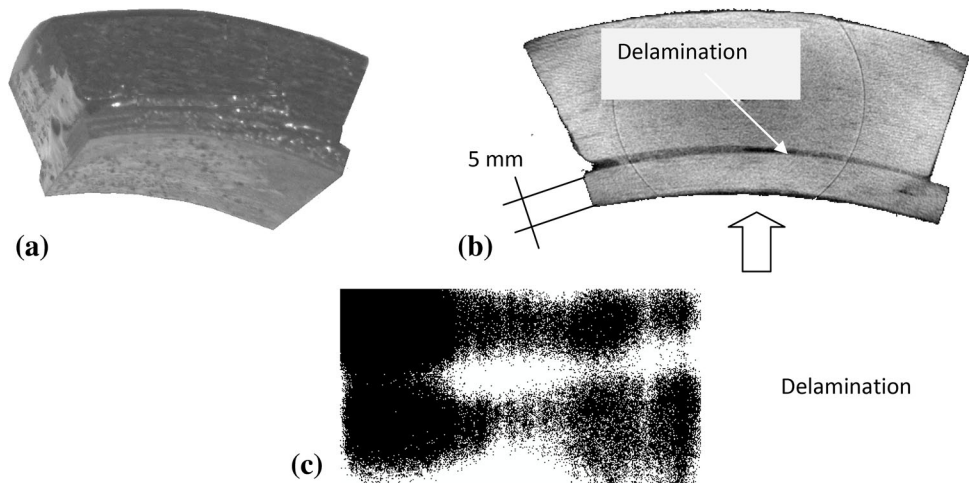
Fig. 4 Detecting the presence of water in aviation honeycomb panels: **a** GFRP skin with aluminum cells and 8 g of water content (*left*-X ray radiographic image, *right*-IR thermogram), **b** Toupolev-204 aileron, approximate water content 120 g (*left* is a UT image, *right* is an IR thermogram)
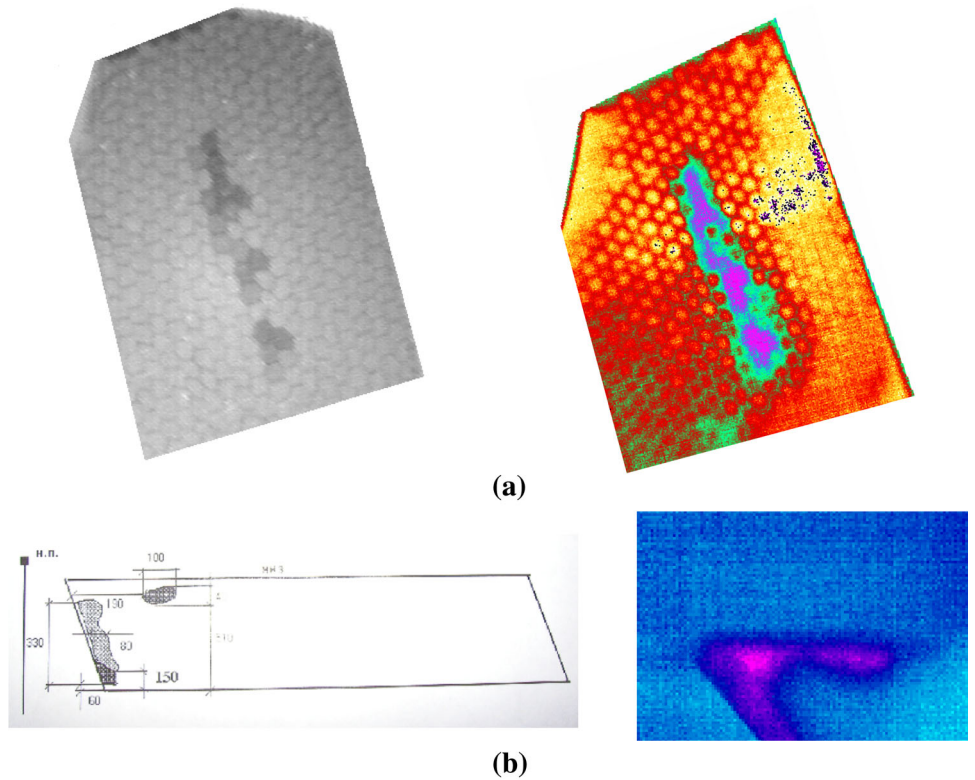
An ultrasonic map of water trapped in a honeycomb reinforced Russian Toupolev-204 airplane part, shown in Fig. 4b, left, took 2 hours to produce, while the IR image in Fig. 4b, right, was taken in just a few seconds.

4.3 Shearography and Thermography

SNDT (Shearographic NDT) uses a laser interferometric technique to create an image of the surface showing out-of-plane displacements, which are caused by the presence of sub-surface anomalies. The excitation for SNDT may be provided by a pressure differential, a thermal pulse, mechanical loading, or vibration. Defects in a composite (or other) material generally have different mechanical properties from those of the surrounding material. The most important mechanical property is stiffness (modulus). The stiffness of the material over a defect is reduced compared to the surrounding material, because the material thickness over a defect is less than the full thickness (as in a delamination). Or the material is disbonded from a reinforcing material, such as honeycomb or foam core. Differences in these properties usually result in differences in the displacement distribution on a surface that provide a shearographic image of the defect.

The amplitude and duration of the mechanical excitation pulse required to make the defect visible depend on the material properties and thickness of the material being inspected.

No single excitation method works for all applications. The effectiveness of SNDT generally decreases with increasing material thickness and increasing stiffness. The inspection of relatively soft, compliant materials is generally very successful using any of several excitation techniques. The inspection of very thick or very stiff materials is generally less successful. However, both thick and stiff materials have been successfully tested by SNDT using special techniques. For example, the SNDT inspection of a thick composite tube has been accomplished by increasing the pressure of the air inside the tube.

A combined TNDT/SNDT system would provide successful inspections on a larger number of material combinations than either method separately (Fig. 5). The two methods complement one another well, and share the characteristics of good portability, relatively high scanning rate, and the fact that several excitation methods may be used for both methods.

1. One method complements the other and provides a "second opinion" to verify the results of the first method used.
2. While each of the techniques may find defects on a particular composite structure, each may show types or sizes of defects that the other does not.
3. Each technique may provide different information about a defect, or about the structure in the vicinity of a defect.
4. Several excitation techniques can be used for both techniques. These include heating by Xenon flash lamp, hot air, or radiation using quartz lamps.

Vacuum excitation, which has been frequently used for SNDT, can also be used to benefit TNDT. The vacuum can be used to separate "kissing" disbonds and, while they are separated, the surface may then be heated to image the disbonds by TNDT.

4.4 Acoustics, Digital Image Correlation and Thermography

Acoustic emission occurs during mechanical testing because microscopic damage is taking place. However, since the damage is minor or insignificant to the function of the part, it is generally considered to be an NDT technique. Carpenter et al. [16] added it to their "big five" list of important NDT methods.

Every thermal event, associated with a local variation of the surface temperature, is the signature of a damaging mechanism, such as delamination or matrix cracking, and can be spatially located, at least in 2D [24,25]. Advanced processing methods, commonly used to improve the contrast of defects detected by flash thermography, can even be applied in order to generate one unique map, by imaging all damaged zones [26].
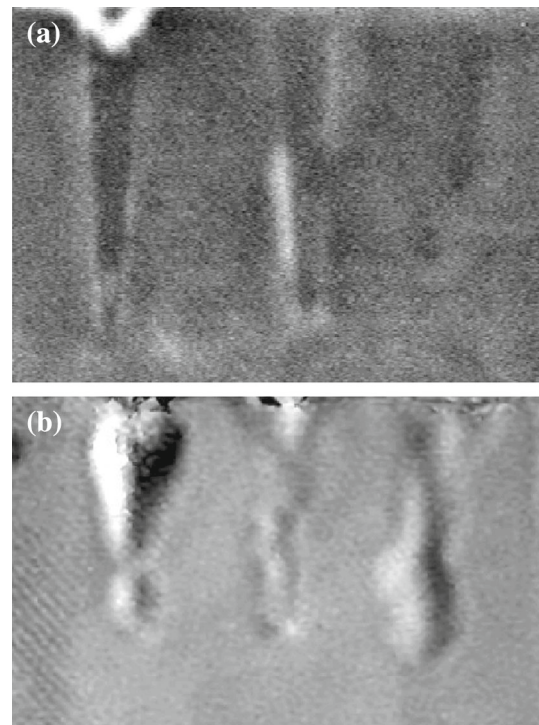
Fig. 5 TNDT (**a**) and SNDT (**b**) images of metal shims implanted in a graphite epoxy laminate [19]

In order to provide an estimation of damage depths, it is useful to compare the data obtained from passive thermography to those from other techniques. One of these can be digital image correlation, which enables the monitoring of the displacement fields of a mechanically loaded structure, and another is acoustic emission, which records all acoustic events that occur during the test. When damage is detected on both the thermal image and the corresponding displacement field, it can be assumed that the defect is nearby the surface. Or, if it is only detected by thermography, it is assumed that the defect is deep enough to have no local influence on the displacement fields. These assumptions can be validated by comparing the time-evolutions of the local temperature variations induced by the damage and the records of the acoustic emission. If the thermal and acoustic signatures are simultaneous, it suggests that the particular defect is shallow; but if the thermal signature is delayed in regard to the acoustic one (which is assumed to be instantaneous), it suggests the presence of a deeper defect. This time delay $\Delta\tau$ is related to the propagation of thermal energy traveling from the buried source to the sample surface. If the thermal observation is limited only to early times after the acoustic emission detection, the experimental temperature profile is similar to the rear-surface response of a plate heated on the front surface by a flash (with no surface heat loss). The normalized temperature signals can then be analyzed similarly to what is commonly done for classic rear-face experiments [27], which leads to
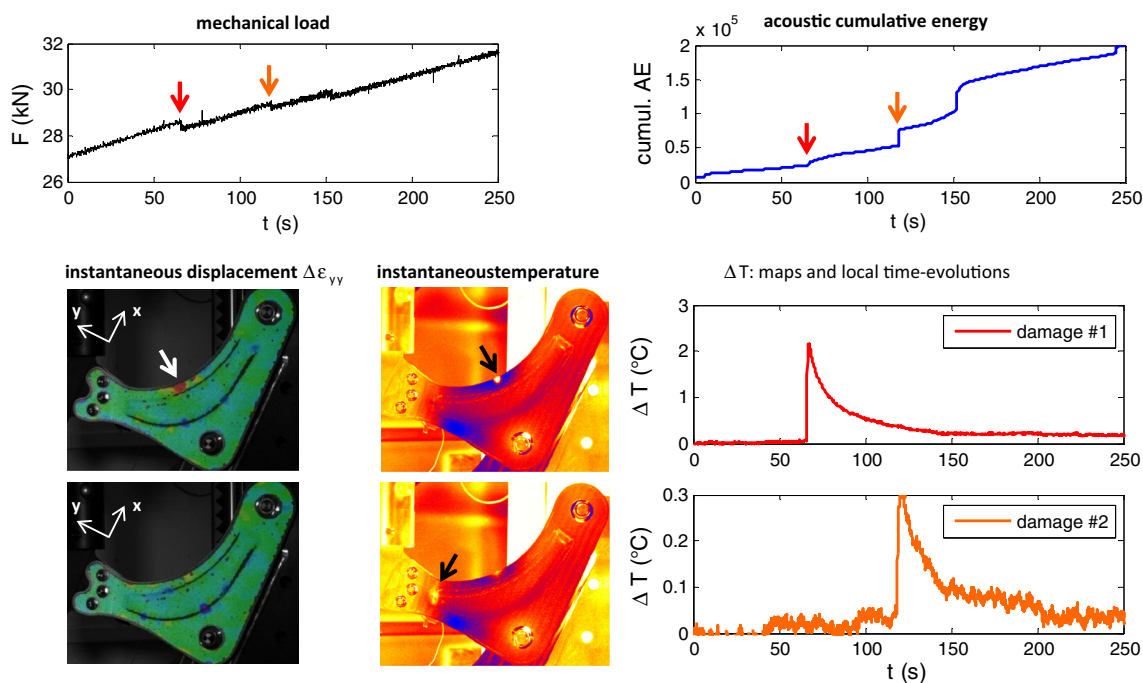
Fig. 6 Detecting damage events in a composite suspension arm during mechanical loading by using passive IR thermography, digital image correlation and acoustic emission

an estimation of the defect depth, assuming that the thermal diffusivity is known.

An illustration of the beneficial combination of passive thermography, digital image correlation and acoustic emission is shown for a multi-instrumented tensile test performed at ONERA, France, on a composite suspension arm [28]. The structure is few millimeter thick and 400 mm long. Mechanical loading is applied with a 15 kN electromechanical Zwick machine. The same face of the suspension arm is observed with two CCD cameras, intended for performing digital image correlation, and by a FLIR X6540sc mid-wavelength IR camera, used for thermal in situ monitoring. IR monitoring is done at an acquisition rate of 10 Hz.

Several piezoelectric sensors are stuck to the opposite face of the structure to enable acoustic monitoring.

Figure 6 shows typical thermal maps and thermograms which are associated with damage occurring during mechanical loading. Two examples are considered: the first damage is seen on both thermal and displacement fields, while the second damage is undetected by digital image correlation. The assumption can be made that damage #1 is a surface defect, while damage #2 is deeper. The local analysis of the thermograms (Fig. 7) validates this assumption. For damage #2, a time delay $\Delta\tau_2$ is checked between the beginning of the temperature variation and the associated acoustic peak. The through-thickness thermal diffusivity of the composite was experimentally determined to be 0.61 ± 0.03 mm^2 s^{-1}, and the depth of the defect can be calculated to be 2.0 ± 0.2 mm. This might explain why this damage is not

seen on the surface displacement fields provided by digital image correlation. As for damage #1, the rise of temperature is almost simultaneous with the acoustic peak, being so fast that an early-time analysis of the thermogram does not seem feasible, even at a higher acquisition frequency. It can still be observed that the first point of the thermogram emerging from the noise, with a normalized temperature increase $\Delta T/\Delta T_{max} = 0.7$, occurs at 0.1 s after the acoustic peak, which is 10 times faster than the occurrence time of the same normalized temperature increase for damage #2. Consequently, the corresponding depth should be roughly $\leq \sqrt{10}$ = 3.16 times shorter than the one of damage #2, i.e. around half a millimeter.

4.5 Ultrasonic and Thermography

As discussed above, UT is among the "Big Five" NDT methods and is often used as a standard against which other NDT methods are compared. A comparison between ultrasonic (UT) and TNDT is provided for one application. In this case study, 140 Kevlar plates of 5 mm thickness were impacted with an indenter using various levels of energy simulating minor to severe impact damage. The plates were inspected by two methods, immersion C-Scan (at 5 MHz), and TNDT, using a 250 W halogen lamp and a FLIR E8-type of IR camera (320 × 240 microbolometer array), shown in Fig. 8.

Compared to the TNDT image, the UT image is less defined but it required about an hour to produce, while the

Fig. 7 Local analysis of the normalized data acquired from passive IR thermography and acoustic emission recording for two detected damages (*left* shallow damage; *right* defect at an estimated depth of 2 mm)
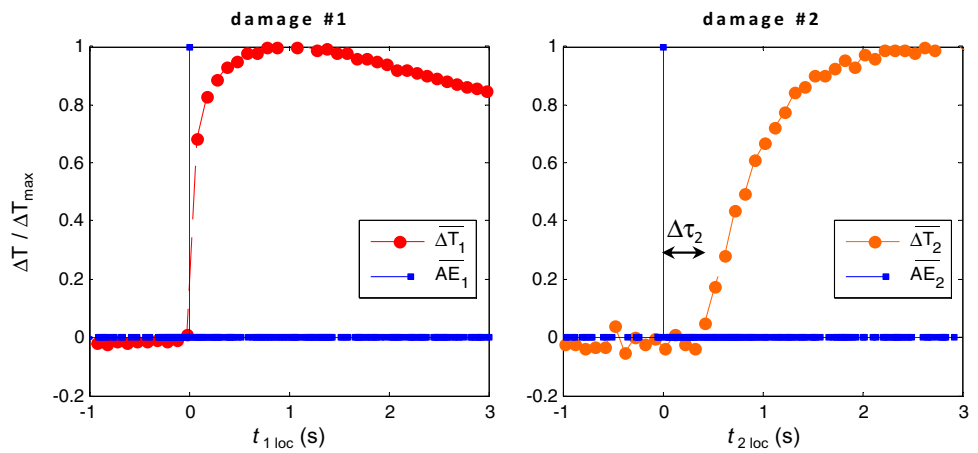
Fig. 8 TNDT setup in transmission (*top left*). Typical recorded thermogram at peak contrast, the typical "butterfly-shaped" delamination is clearly visible (*top right*). Corresponding 5 MHz C-Scan UT (*bottom*). Images courtesy of P. Servais (NDT Pro) [29]
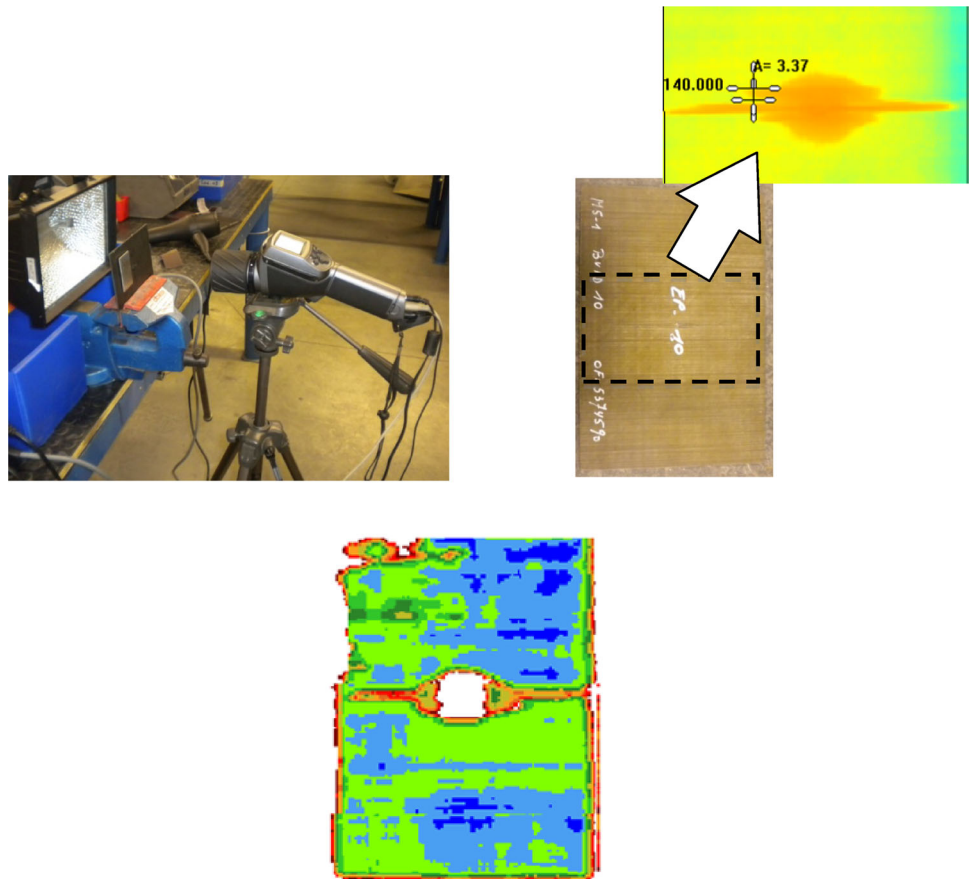

TNDT inspection was achieved in ~5 s. A subsequent POD (Probability of Detection) analysis was performed (using the HIT-MISS approach) and revealed a $a_{90,95}$ of 7.81 mm for TNDT and 12.75 mm for UT [29,30]. The $a_{90,95}$ criteria requires that a feature (here the diameter of a potential defect) must be detected with a 90 per cent probability and with 95 per cent confidence. In this example, TNDT performed better than UT since it enabled the detection of smaller (7.81 mm) defects than UT (12.75 mm). This result is typical of recent progress in TNDT and clearly demonstrates its attrac-

tiveness. It is important to note, however that POD analyses are not generally applicable; they are specific to a single set of test conditions. Other conditions, components, and equipment will provide different values of $a_{90,95}$.

4.6 3D Measurement and Thermography

In some cases, it is useful to combine thermographic inspection results with a image of the sample: thermography shows defects, but the sample geometry may be not easily recog-
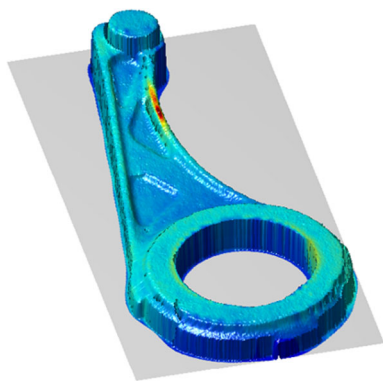
Fig. 9 3D data merged with thermographic results (the crack at the arm lever becomes visible due to the higher temperature)

nizable in the image, thus making it difficult to identify the location of the defects. Often, the sample geometry affects thermographic results, as the heat may accumulate at the edges and corners of the sample. A combined evaluation of visual data and the corresponding IR image can help avoiding false failure detection, as well as aiding in marking the location of the defect on the surface of the part.

Figure 9 shows a fused image of an arm lever, The 3D data was obtained by applying the "light-sectioning" technique and the IR image was recorded after a short period of induction heating (see Sect. 5.2) [31]. The two data sets are superimposed. The forging lap is easily visible at the lever arm due to the higher temperature increase.

Note that, when merging thermographic data with visible images of the sample, one has to take into account the dependence of the emissivity, as well as reflectivity, from the viewing direction.

5 Novel Techniques Resulting from the Integration of TNDT with Other Technique

5.1 Vibrothermography

A general name of this technique is vibrothermography and, depending on the vibrational frequency used, it may be called ultrasonic, or sonic, IR thermography. A very attractive fea-

ture of this technique is that thermal energy is generated only by structural inhomogeneities (possible defects) while homogenous (non-defect) areas remain relatively unchanged (if no significant mechanical hysteresis occurs in the material being tested). Vibrothermography, proposed in the 1970s [32,33], has been intensively explored since then [34–39]. The disadvantages of this technique are that the stimulation requires contact with the sample and the high power required may cause damage, especially at the contact point.

Since this method is explained extensively in many papers, we will limit ourselves to one example in which IR thermographic results, obtained by applying both optical and ultrasonic stimulation, are fused to detect impact damage in CFRP (Carbon Fiber Reinforced Plastic). Figure 10a shows the surface temperature signature of impact damage section which is characterized by significant thermal resistance (thickness). Ultrasonic stimulation causes frictional heating inside very thin defects (Fig. 10b); one can also talk about considering the possibility of detection of "kissing disbonds". A simple fusion technique, imposing source images with varying image (%) transparency, allows a more general presentation of the impact damage (Fig. 10c).

In another example, Fig. 11 shows inspection results of an aircraft (CF18 military jet) rudder, which contains two delaminations. Both vibrothermography and conventional flash thermography were used. In this case, the thermal contrast was much higher for vibrothermography due to the amount of energy injected in the specimen [40].

Vibrothermography is a good TNDT approach especially for the detection of cracks and "kissing disbonds", and for metal or ceramic specimens. It is best applied to hard materials, rather than more fragile, softer materials such as composites (CRFP and other), since the vibration and contact pressure between the sonotrode (transducer) and the specimen might cause wear or other damage to the specimen.

This is not the case for metal components [41,42].

Ultrasonic thermography is still being developed, in particular to reduce the mechanical energy required, as this may be necessary to make tests truly nondestructive without losing sensitivity for defect detection. To reduce the energy input, frequencies may be used which produce resonance in the defect [43]. Another approach for large plate-type

(a)   **(b)**   **(c)**
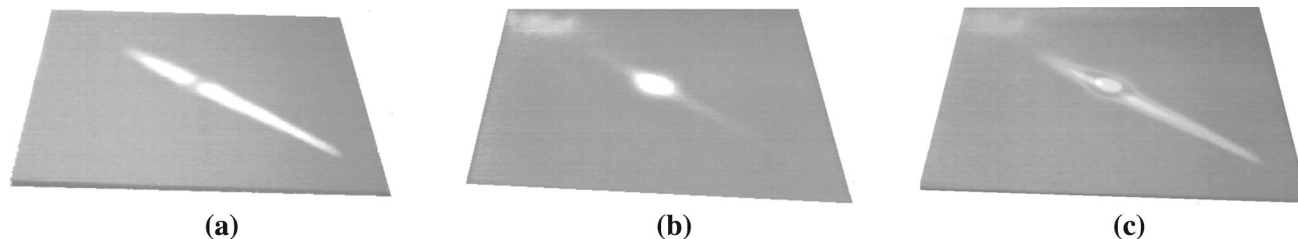
Fig. 10 Detecting impact damage in CFRP: **a** flash optical stimulation (the main body of damage is seen), **b** ultrasonic stimulation (the area around the impact is seen), **c** fusion of IR thermograms from (**a**) and (**b**)
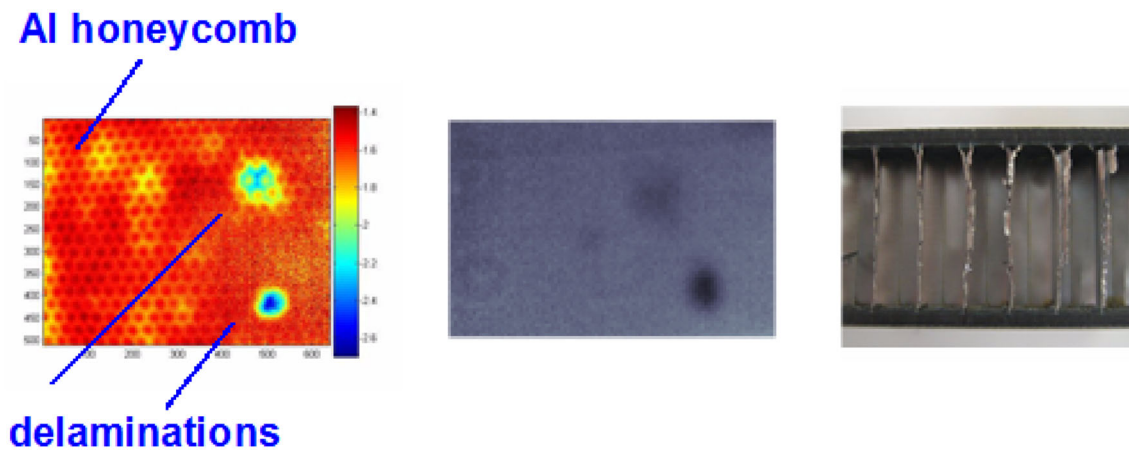
Fig. 11 CF18 rudder inspection. Aluminum honeycomb (4 cm) with CFRP skins (2 mm) [40]. Thermogram obtained after vibrothermography (*left*). Corresponding flash thermography image (*center*). Specimen cross-section (*right*)

structures and detection at long distances consists of using frequencies that create Lamb waves [44].

5.2 Induction Heating Thermography

To use induction heating for thermography, a specimen is placed inside an induction coil and a short electric pulse from 50 ms to 1 s is applied. When defects disturb the distribution of the eddy current, as well as the heat flow, they become visible in the IR image. This technique can be used for testing electrically conductive materials, such as metals, but it can also work for CFRP [45]. Inductive heating is especially effective for ferromagnetic steel, in which the induced eddy current is very high due to the high magnetic permeability [46]. As with Joule heating, which is caused by the electrical resistance of the material, inductive heating is generated inside the sample. A low, or non-uniform, absorption coefficient for inductive heating creates much less thermal disturbance than optical (radiation) heating of a surface, where the heat has to be first absorbed by the surface itself.

This technique can be used to detect subsurface defects or even to evaluate the quality of welded or adhesively bonded joints [47–49], both in reflection or in transmission mode. However, the primary application is detecting surface cracks [46–52].

In the early 1980s, a commercial test instrument, called the Therm-O-Matic [53], was offered for detecting surface cracks in steel bars and billets. Long objects were moved at a speed of about 1 m/s through an induction coil and four line-scanning IR cameras monitored the whole sample surface.

In the last few years, a couple of new applications have been developed, mainly to detect surface cracks in forgings, castings, wires and in other metal products [50–54]. For most of these applications, standard NDT techniques,

such as magnetic particle, eddy current or liquid penetrant are used. However, induction thermography is becoming increasingly popular since it is faster. Also, this technique can be fully automated for determining the depth of surface cracks, [55].

Figure 12 shows a typical example of detecting shallow surface cracks in a steel sample. Instead of evaluating one single temperature image, a Fourier phasegram calculated from the whole image sequence was used to essentially eliminate surface clutter [56]. Image processing can be automated to localize cracks.

Figure 12c shows the same sample with fluorescent magnetic particle testing. In this case, the crack is less obvious, thus making its automated detection very difficult.

Another approach for inductive thermography is to position a small inductive coil at a fixed distance away from the specimen. When energized, the coil generates Eddy currents in electrically conductive specimens (Steel, Aluminum, CFRP, etc.). A defect, such as a crack, acts as an electrical resistor, and the passage of the induced electric current through this may generate sufficient Joule heating to a create temperature "signature" that is detectable by an IR camera [57]. Fig. 13 illustrates the approach.

As stated previously, heat transfer problems in TNDT are extensively documented [58] and thermal modeling can be performed with finite element packages such as ABACUS or COMSOL. An example of such modeling is shown in Fig. 14 for the case of the inductive thermography example in Fig. 13. Heating of the crack by the nearby coil is clearly demonstrated. Modeling is convenient to optimize experimental parameters such as the number of turns for the coil, the amplitude of the current in coil, the scanning speed, and space between the coil and the surface. Obviously, this can save a tremendous amount of experimental time in the laboratory.

Fig. 12 Steel fitting with a crack in an area that was ground down: **a** sample photo, **b** Fourier phasegram IR image, calculated after a short inductive heating pulse (the crack is easily visible in the ground region), **c** same sample photo after magnetic particle testing (the crack is slightly visible in the middle of the image)

(a)

(b)

(c)
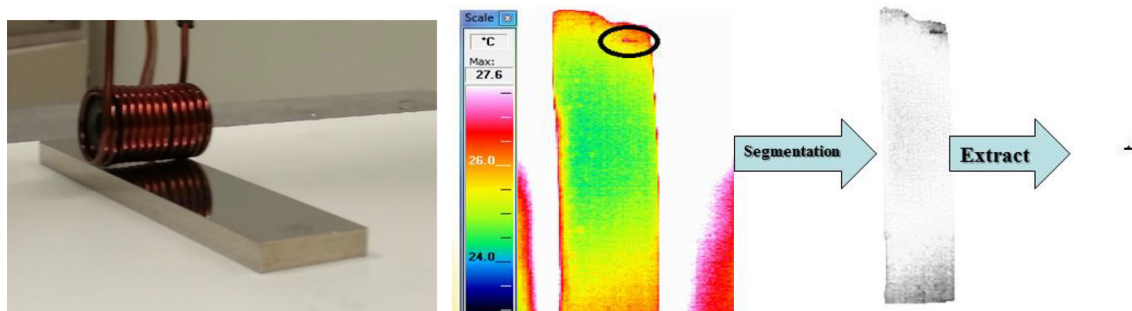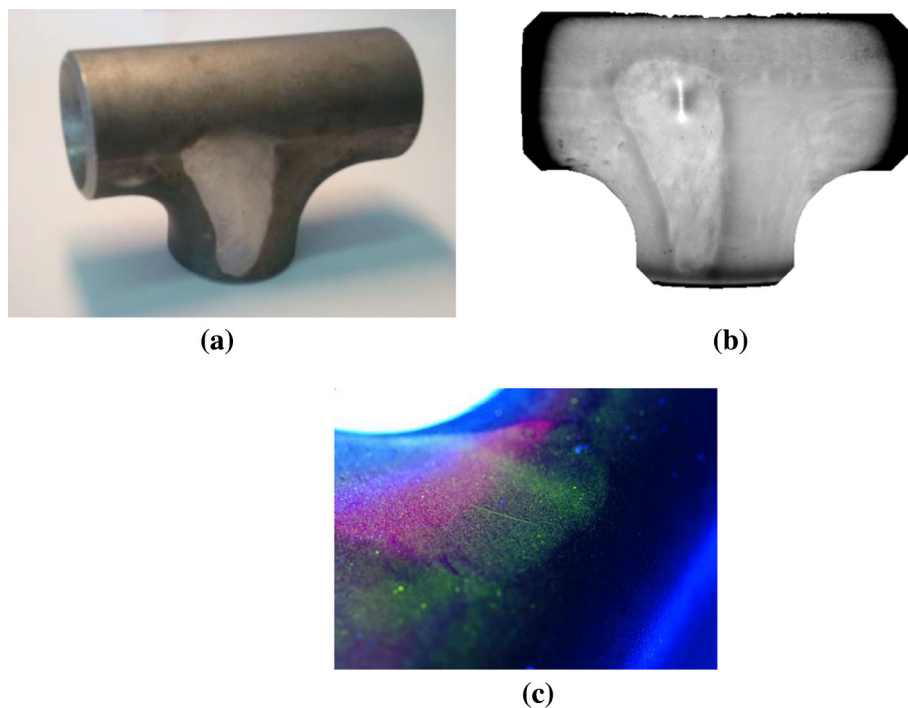
Fig. 13 Inductive thermography performed by scanning a small coil over a steel specimen. Picture of the coil over a steel specimen (*left*). TNDT inspection showing raw and processed thermograms with extracted crack highlighted [57]

Fig. 14 Inductive thermography: Finite Element Modeling heating of the crack by a nearby inductive coil shown in Fig. 13 (*left*) is shown on the right. Here COMSOL was used
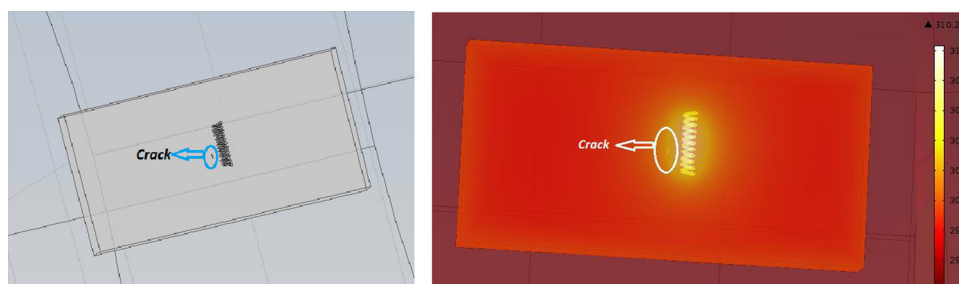
5.3 Electromagnetic-Infrared (EMIR) Thermography

Implementation of FPA (Focal Plan Array) IR cameras, which allow the simultaneous recording of the temperature-time histories of hundreds of thousands (recently increased to a million) points on the tested structure surface, may produce a dramatic increase of productivity compared to methods based on other physical phenomena, such as radar or terahertz radiation. This is possible if a photothermal converter is coupled to the IR camera. This idea is not new, dating back to the 1950s [59] and was applied for the first time using an IR camera in the 1970s [60]. In the following decades, some basic research on visualization of microwaves (from W-band [61] to X-band [62]) was performed by Sega and colleagues
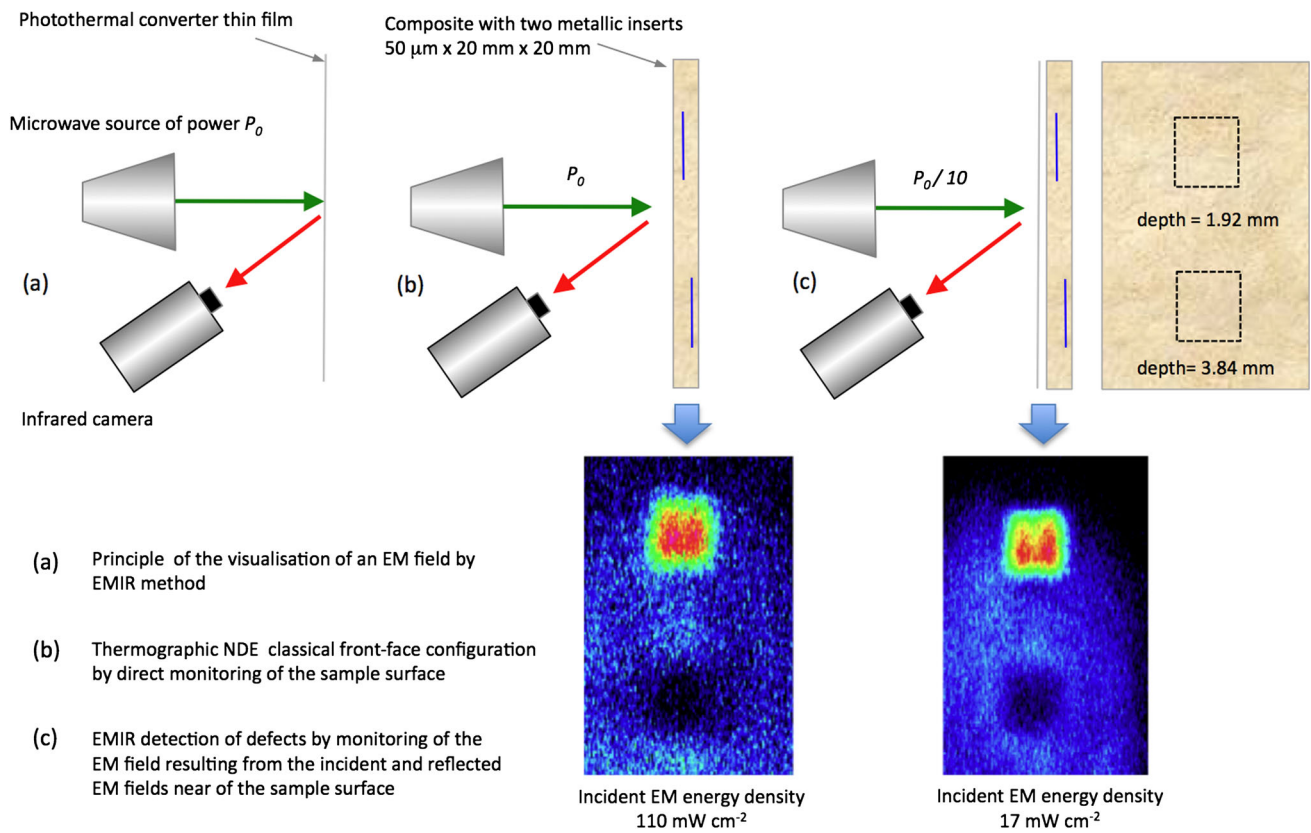
Fig. 15 Visualizing the intensity of an X-band (centimeter wavelength) electric field by using an IR camera and a photothermal converter (thin electrically-conductive film); application to defect imaging in a carbon-loaded glass/resin composite; comparison to the direct observation of the sample surface temperature. (adapted from [59]). Note that the better image of the defects, on the right, is obtained with less excitation energy and when using the converter film as shown in the diagram above it. The IR image on the left is without the converter, as shown in the diagram above it

at the Colorado University in Colorado Spring and in the 90's at ONERA (in Ku and X bands [63]). Typically, the converter is a thin polymeric film (a few tens of microns thick) made electrically-conductive by a coating or by loading with carbon particles. Mounted in a radar field, the film absorbs a part of the electric field and the map of its temperature increase reveals the distribution of electromagnetic intensity in the plane of the film (see Fig. 15a).

For NDT purposes, the use of such a film (in a method like the one described in Sect. 4.1 or the one presented in Fig. 15b), produces a dramatic change in the defect signature, as seen in Fig. 15c (improved signal-to-noise ratio and sharpness). This is because the thermal image of the converter film recorded by the camera is not affected by the 3-D heat diffusion in the structure. That thermal image results from the addition of the incident and reflected electromagnetic fields. The defect signature corresponds to differences in electrical permittivity of the structure and the defect.

When applied to composites, this method is adapted to defects that are more electrically conductive than the host material [63]. Therefore, it works well for detecting water in composites and honeycomb sandwich panels [64]. It has been also applied to radar-absorbing composite materials [65], as well as in mine detection [66].

5.4 Terahertz–Thermography

The same approach as in the preceding section can be applied to terahertz stimulation [67,68], as the EMIR film has an extremely wide range, going from visible to radio frequency. To illustrate this, some results of incident multispectral wave measurements are shown in Fig. 16.

An important advantage of terahertz radiation in comparison with X rays is that its non-ionizing properties present no danger to personnel. It can be assumed that all thermally-insulating materials, such as plastic, wood, etc., are transparent in the THz (millimeter wavelength) wavelength band. Conversely, metals behave as a mirror while water and carbon are perfect absorbers. Therefore, this technique can be used in a transmission mode for all thermally-insulating materials and in a reflection mode for other materials. An example of detecting water in a plastic honeycomb structure is shown in Fig. 17 [69].
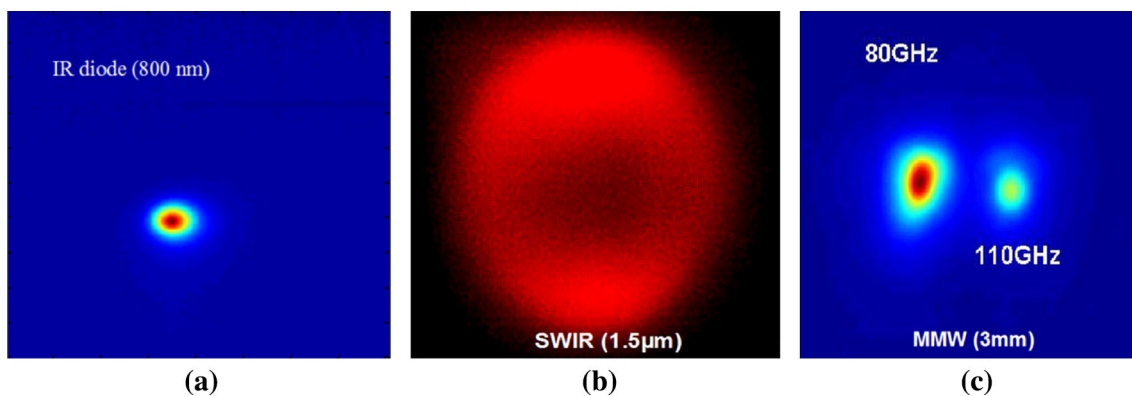
Fig. 16 Some results of incident multispectral wave measurement: **a** IR laser diode at 800 nm, **b** IR source at 1.5 μ*m*, and **c** two THz sources at around 3 mm
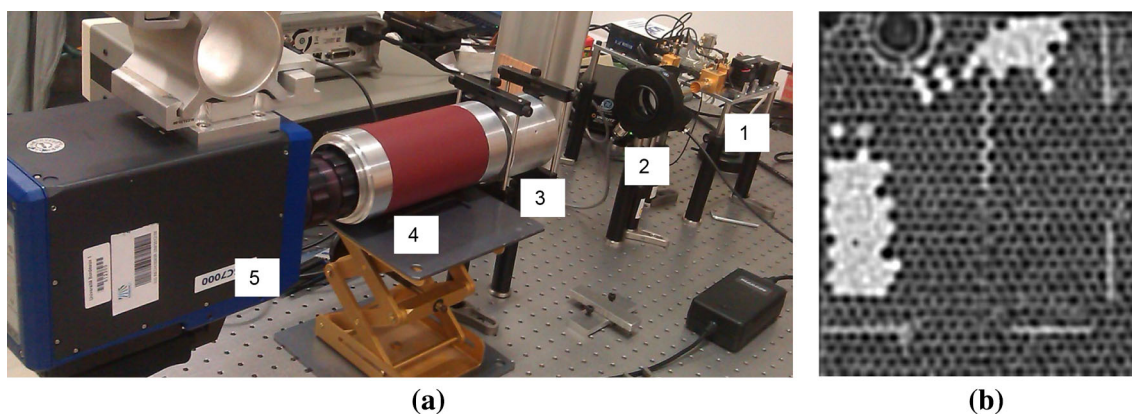
Fig. 17 Detecting water in a plastic honeycomb structure: **a** experimental setup, set-up (*1*—110GHz Gunn diode, *2*—mechanical shutter, *3*—THz objective, *4*—THz-IR objective with Tera Thermal Converter, *5*—IR camera) and **b** IR thermogram of plastic honeycomb structure with two water-filled areas

The technique of THz IR thermography seems to be effective in monitoring drying processes and the detection of metallic objects in thermal insulators, the latter of which is difficult by applying "classical" thermal NDT.

are also possible in TNDT, especially when using the pulsed mode [70].

The above references provide additional details, including the wide body of literature published on this topic [75].

6 Image Processing

It is important to state that image processing is essential for TNDT, since raw images rarely display defects [70]. In the basic but interesting "thermal contrast" technique, a defect-free or cold reference image is sustracted from thermograms of interest. Now, more complex approaches such as Differential Absolute Contrast (DAC) [71], Thermographic Signal Reconstruction (TSR) [72], Principal Component Thermography (PCT) [73], Pulsed Phase Thermography (PPT) [56] and more recently, Partial Least Square Thermography (PLST) [74] are used to increase defect detectability in TNDT. As a result, their use is recommended for many applications.

Also, the quantitative evaluation of defect depth and size as well as the determination of thermal properties of materials

7 Conclusions

- Due to its underlying physical principles, TNDT may be considered to be a more universally applicable NDT method compared to more traditional NDT techniques, such as X ray, ultrasonic, eddy current, and liquid penetrant. It can be applied to both metals and non-metals to detect defects such as cracks, foreign object inclusions, disbonds, delaminations, variations in thermal properties, etc.
- The effectiveness of TNDT depends on a combination of thermal and optical properties which provide both advantages and disadvantages of the technique. IR thermograms represent surface temperature distributions and also show variations in material optical (absorption/emissivity) properties. But TNDT test results can be

negatively affected by surface clutter and thermal noise. Therefore, by combining thermal method with other NDT techniques, one may take advantage of both.

- In particular, for composite materials, TNDT is more efficient and productive than most other techniques, and is especially useful for screening purposes. TNDT test results may be processed by advanced algorithms that had been developed in other areas. The TNDT technique is also remote and safe.
- Novel TNDT techniques, such as ultrasonic and eddy current IR thermography, have successfully detected defects such as "kissing disbonds" and surface cracks, which were not previously detectable by"classical" TNDT.
- Since heat is a basic form of energy transmission, we can agree with L.Z. Kriksunov that thermography applications are only limited by our imagination [76]. This is illustrated in Sect. 5.

References

1. Green, D.R.: An instrument for nondestructively testing fuel core to cladding heat transfer. Nucl. Sci. Eng. **12**, 271–277 (1962)
2. Green, D.R.: Emissivity-independent infrared thermal testing method. Mater. Eval. **23**(2), 79–85 (1965)
3. Beller, W.S.: Navy sees promise in infrared thermography for solid case checking. Missiles Rockets **22**, 1234–1241 (1965)
4. Carlomagno, G.M., Berardi, P.G.: Unsteady thermophototopography in nondestructive testing. In: Proceedings of 3rd biannual exchange, St. Louis, pp. 33–39. (1976)
5. Rosencwaig, A., Gersho, A.: Thermal-wave imaging. Science **218**, 223–228 (1982)
6. Vavilov, V.P., Taylor, R.: Theoretical and practical aspects of the thermal NDT of bonded structures. In: Sharpe, R.S. (ed.) Research Techniques in NDT, vol. 5, pp. 239–279. Academic Press, London (1982)
7. Cielo, P.: Pulse photothermal evaluation of layered materials. J. Appl. Phys. **56**(1), 230–234 (1984)
8. Almond, D., Patel, P.: Photothermal Science and Techniques. Chapman & Hall, London (1996)
9. Willburn, D.K.: Survey of infrared inspection and measurement techniques. Mater. Res. Stand. **1**, 528 (1961)
10. McGonnagle, W., Park, F.: Nondestructive testing. Intern. Sci. Technol. **7**, 14 (1964)
11. Burleigh, D.: A bibliography of nondestructive testing (NDT) of composite materials performed with infrared thermography and liquid crystals. In: Proceeding of SPIE Thermosense-IX, vol. 780, pp. 250–255 (1987)
12. Maldague, X.:Theory and Practice of Infrared Technology for Nondestructive Testing. Wiley Series in Microwave and Optical Engineering. Wiley, New York (2001)
13. Balageas, D.L., Krapez, J.-C., Cielo, P.: Pulsed photo-thermal modeling of layered materials. J. Appl. Phys. **59**(2), 348–357 (1986)
14. Vavilov, V.P., Burleigh, D.D.: Review of pulsed thermal NDT: physical principles, theory and data processing. NDT E Int. **73**, 28–52 (2015)
15. Vavilov, V.: Thermal NDT: historical milestones, state-of-the-art and trends. Quant. Infrared Therm. J. **11**(1), 66–83 (2014)
16. Carpenter J.L., Stuhrke W.F. (1976) NDE - An effective approach to improved reliability and safety. A technology survey, Martin Marietts Corporation, Orlando, Florida, USA, N76 25375 (NASA CR 134963): 178
17. Cawley, P.J.: Non-destructive testing–current capabilities and future directions. J. Mater. Des. Appl. **215**, 213–223 (2001)
18. Cramer, K., Winfree, W., Hodges, K., Koshti, A., Ryan, D., Reinhard, WW.: Status of thermal NDT of space shuttle materials at NASA. In: Proceedings of SPIE "Thermosense-XXVIII", vol. 6205, p. 62051B1-9 (2006)
19. Burleigh D.A.: Portable, combined thermography/shearography NDT system for inspecting large composite structures. In: Proceeding of SPIE "Thermosense-XXIV" vol. 4710, pp. 578–587 (2002)
20. Winfree, W.P.: Enhanced Thermographic Detection of Delaminations with Computational Pulse Shaping. Rev of Progress in Quant NDE, pp. 441–448. New York, Plenum Press (1998)
21. Pilla M., Galmiche F., Maldague M.: Thermographic inspection of cracked solar cells. In: Proceedings SPIE "Thermosense XXIV", vol. 4710, pp. 699–703 (2002)
22. Swiderski, W., Nesteruk, D.A., Vavilov, V.P., Derusova, D.A.: Data fusion in IR thermographic detection of landmines and NDT of composites. Atti della Fondazione Giorgio Ronchi, Anno LXIX, Edizione Tassinari, Firenze, Italy **4**, 473–478 (2014)
23. Grosso, M., Marinho, C.A., Nesteruk, D.A., Rebello, J.M., Soares, S.D., Vavilov, V.P.: Evaluating quality of adhesive joints in glass fiber plastic piping by using active thermal NDT. In: Proceedings of SPIE "Thermosense-XXXV", vol. 8705, p. 87050T (2013)
24. Roche, J.-M., Lamboul, B., Grail, G., Osmont, D., Balageas, D.: Thermal and ultrasonic damage monitoring and characterization in woven composites. In: 19th International Conference on Composite Materials (ICCM 19), Montreal, 2–11 (2013)
25. Balageas, D., Levesque, P., Brunet, P., Cluzel, C., Déom, A., Blanchard, L.: Thermography as a routine diagnostic for mechanical testing of composites. Quant. InfraRed Therm. J. **5**(1), 45–68 (2008)
26. Balageas, D., Roche, J.-M., Leroy, F.-H., Liu, W.-M., Gorbach, A.: The thermographic signal reconstruction method: a powerful tool for the enhancement of transient thermographic images. Biocybern. Biomed. Eng. J. **35**, 1–9 (2015)
27. Balageas, D.: In search of early time. An original approach in the thermographic identification of the thermophysical properties and defects. Adv. Opt. Technol. doi:10.1155/2013/314906
28. Roche, J.-M., Passilly, F., Leroy, F.-H., Lapeyronnie, P., Fagiano, G.: Thermal non-destructive characterization and in situ damage monitoring of a composite suspension wishbone. PhotoMechanics Conference, Delft (2015)
29. Duan, Y., Servais, P., Genest, M., Ibarra-Castanedo, C., Maldague, X.P.V.: ThermoPoD: a reliability study on active infrared thermography for the inspection of composite materials. In: International Conference Materials and Reliability (ICMR 2011), Busan, Korea (2011)
30. Duan, Y., Servais, P., Genest, M., Ibarra-Castanedo, C., Maldague, X.P.V.: ThermoPoD: a reliability study on active infrared thermography for the inspection of composite materials. J. Mech. Sci. Technol. **26**(7), 1985–1992 (2012)
31. Oswald-Tranta, B., O'Leary, P.: Fusion of geometric and thermographic data for automated defect detection. J. Electron. Imaging **21**(2), 021108–021118 (2012)
32. Henneke, E.G., Reifsnider, K.L., Stinchcomb, W.W.: Thermography, an NDI method for damage detection. J. Met. **31**(9), 11–15 (1979)
33. Pye, C.J., Adams, R.D.J.: Heat emission from damaged materials and its use in nondestructive testing. J. Phys. D **14**, 927 (1981)

34. Mignona, R.B., Green Jr, R.E., Duke Jr, J.C.: Thermographic investigation of high-power ultrasonic heating in materials. Ultrasonics **19**, 159–163 (1981)

35. Zweschper, T., Dillenz, A., Busse, G.: Ultrasound lock-in thermography: a defect selective method for the inspection of aerospace components. Insight **43**, 173–179 (2001)

36. Morbidini, M., Cawley, P., Barden, T., Almond, D.: Prediction of the thermosonic signal from fatigue cracks in metals using vibration damping measurements. J. Appl. Phys. **100**, 104905 (2006). doi:10.1063/1.2361091

37. Morbidini, M., Cawley, P.: A calibration procedure for sonic infrared nondestructive evaluation. J. Appl. Phys. **106**, 023504-1–023504-7 (2009)

38. Holland, S.D., Uhl, C., Ouyang, Z., Bantel, T., Li, M., Meeker, W.Q., Lively, J., Brasche, L.: Quantifying the vibrothermographic effect. NDT E Int. **44**, 775–782 (2011)

39. Guo, X., Vavilov, V.P.: Crack detection in aluminum parts by using ultrasound-excited infrared thermography. Infrared Phys. Technol. **61**, 149–156 (2013)

40. Sfarra, S., Ibarra-Castanedo, C., Avdelidis, N.P., Genest, M., Bouchagier, L., Kourousis, D., Tsimogiannis, A., Anastassopoulous, A., Bendada, A., Maldague, X., Ambrosini, D., Paoletti ,D.: A comparative investigation for the nondestructive testing of honeycomb structures by holographic interferometry and infrared thermography. 15th ICPPP, 24–28 July 2009, Leuven, Belgium. Publication. In: Journal of Physics: Conference Series 214 (2010): 012071 (2009)

41. Ibarra-Castanedo, C., Piau, J.-M., Guilbert, S., Avdelidis, N.P., Genest, M., Bendada, A., Maldague, X.P.V.: Comparative study of active thermography techniques for the nondestructive evaluation of honeycomb structures. Res. Nondestruct. Eval. **20**, 1–31 (2009)

42. Genest, M., Forsyth, D.S., Maldague, X.: Comparison of solid highlighter materials for thermography. CINDE J. **28**(4), 7–12 (2007)

43. Solodov, I., Rahammer, M., Derusova, D., Busse, G.: Highly-efficient and noncontact vibro-thermography via local defect resonance. Quant. Infrared Therm. J. **12**(1), 98–111 (2015)

44. Krapez, J.-C., Taillade, F., Balageas, D.: Ultrasound-lockin-thermography NDE of composite plates with low power actuators. Experimental investigation of the influence of the Lamb wave frequency. Quant. Infrared Therm. J. **2**(2), 191–206 (2005)

45. Riegert, G., Zweschper, T., Busse, G.: Lockin thermography with eddy current excitation. Quant. Infrared Therm. J. **1**(1), 21–31 (2004)

46. Oswald-Tranta, B.: Thermoinductive investigations of magnetic materials for surfacecracks. Quant. Infrared Therm. J. **1**(1), 33–46 (2004)

47. Riegert, G., Gleiter, A., Busse, G.: Potential and limitations of eddy current lockin-thermography. In: Proceedings of SPIE "Thermosense XXVIII", vol. 6205, p. 62051E (2006). doi:10.1117/12.662716

48. Oswald-Tranta, B., Sorger, M.: Detection of subsurface defects in aluminium with thermo-inductive inspection. In: Proceedings of SPIE, "Thermosense XXXIII", vol. 8013, p. 801310 (2011). doi:10.1117/12.887193

49. Oswald-Tranta, B., Sorger, M.: Scanning pulse phase thermography with line heating. Quant. Infrared Therm. J. **9**(2), 103–122 (2012)

50. Oswald-Tranta, B.: Thermo-inductive crack detection. J. Nondestruct. Test. Eval. **22**(2–3), 137–153 (2007)

51. Zenzinger, G., et al.: Thermographic crack detection by eddy current excitation. J. Nondestruct. Test. Eval. **22**(2–3), 101–111 (2007)

52. Wilson, J., et al.: Modelling and evaluation of eddy current stimulated thermography. J. Nondestruct. Test. Eval. **25**(3), 205–218 (2010)

53. Kremer, K., et al.: Das Therm-O-Matic-Verfahren - ein neuartiges Verfahren für die Online-prüfung von Stahlerzeugnissen auf Oberflächenfehler. Stahl Eisen **105**, 39–44 (1985). (in German)

54. Oswald-Tranta, B., Sorger, M.: Localizing surface cracks with inductive thermographical inspection: from measurement to image processing. Quant. Infrared Therm. J. **8**(2), 149–164 (2011)

55. Oswald-Tranta, B., Schmidt, R.: Crack depth determination with inductive thermography. In: Proceeding SPIE "Thermosense XXXVII", vol. 9485, pp. 9485–9512 (2015)

56. Maldague, X., Marinetti, S.: Pulse phase infrared thermography. J. Appl. Phys. **79**(5), 2694–2698 (1996)

57. Tran-Gia, P., Maldague, X., Birglen, L.: Crack detection limit in eddy current thermography. In: ASNT Spring Research Conference, pp. 1–6 (2013)

58. Carslaw and Jaeger: Conduction of Heat in Solids. Clarendon Press, Oxford (1959)

59. Hasegawa, T.: A New Method of Observing Electromagnetic Fields at High Frequencies by Use of Test Paper. Bulletin of Yamagata University IV, Yamagata (1955)

60. Gregoris, L., Iizuka, K.: Thermography in microwave holography. Appl. Opt. **14**(7), 1487–1489 (1975)

61. Sega, R.M., Benkelman, C.A., Norgard, J.D.: Measurements of antenna patterns at 94 GHz using infrared detection. In: Proceedings SPIE "Millimeter Wave Technology III", vol. 544, pp. 234–240 (1985)

62. Norgard, J., Musselman, R.: Direct infrared measurement of phase array near-field and far-field antenna patterns. Quant. Infrared Therm. J. **2**(1), 113–125 (2005)

63. Balageas, D., Levesque, P.: EMIR: a photothermal tool for electromagnetic phenomena characterization. Rev. Gén. Therm. **37**(8), 725–739 (1998)

64. Balageas, D., Bourasseau, S., Dupont, M., Bocherens, E.: Dewynter-Marty V. Comparison between nondestructive evaluation techniques and integrated fiber optic health monitoring systems for composite sandwich structures. J. Intell. Mat. Syst. Struct. **11**, 426–437 (2000)

65. Balageas, D., Levesque, P., Nacitas, M., Krapez, J.-C., Gardette, G., Lemistre, M.: Microwaves holography revealed by photothermal films and lock-in IR thermography: application to electromagnetic materials NDE. In: Proceeedings of SPIE "Aging infrastructure and manufacturing 96 Symposium—Nondestructive evaluation of materials and composites". vol. 2944, pp. 55–66 (1996)

66. Balageas, D., Levesque, P.: Mines detection using the EMIR method. In: Proceedings of QIRT'02 Conference Dubrovnik 24–27, 2002. QIRT Open Archives, http://www.qirt.org/dynamique/index.php?idD=44 (2002)

67. Matveenko, A.N., Medvedev, L.E., Miginsky, S.V., Mironenko, L.A., Ovchar, V.K., Popik, V.M., Salikova, T.V., Scheglov, M.A., Serednyakov, S.S., Shevchenko, O.A., Skrinsky, A.N., Tcheskidov, V.G., Vinokurov, N.A.: Research highlights from the Novosibirsk 400 W average power THz FEL. Terahertz Sci. Technol. **1**(2), 107–125 (2008)

68. Pradere, C., Caumes, J.P., Balageas, D., Salort, S., Abraham, E., Chassagne, B., Batsale, J.-C.: Photothermal converters for quantitative 2D and 3D real-time TeraHertz imaging. Quant. Infrared Therm. J. **7**(2), 217–235 (2010)

69. Chulkov, A.O., Gaverina, L., Pradere, C., Batsale, J.-C., Vavilov, V.P.: Detecting hidden water in honeycomb composite structures by using Terahertz thermography. Russ. J. NDT (2015)

70. Ibarra-Castanedo C., Genest M., Maldague X. (2013) Infrared vision: visual inspection beyond the visible spectrum. Integrated Imaging and Vision Techniques for Industrial Inspection: Advances and Applications, Zheng Liu Ed., Springer, New York (2013)

71. Pilla, M., Klein, M., Maldague, X., Salerno, A.: New absolute contrast for pulsed thermography. Proc. QIRT **2002**, 53–58 (2002)

72. Shepard, S.M.: Advances in pulsed thermography. In: Proceedings of SPIE "Thermosense XXVIII", vol. 4360, pp. 511–515 (2001)
73. Rajic, N.: Principal component thermography for flaw contrast enhancement and flaw depth characterisation in composite structures. Compos. Struct. **58**, 521–528 (2002)
74. López, F., Nicolau, V., Maldague, X., Ibarra-Castanedo, C.: Multivariate signal processing by partial least-squares thermography.

In: Proceedings of 7th IWASPNDE, Quebec, Canada pp. 29–34 (2014)
75. http://www.qirt.orgunderarchives
76. Kriksunov, L.Z.: Handbook on the Basics of Infrared Technique. Sovetskoye radio Publisher, Moscow (1978)